



Broadband White Luminescent Phosphor $\text{Ba}(\text{Si}_{7-x}\text{Al}_x)\text{Li}_y(\text{N}_{10-x+y}\text{O}_{x-y}):\text{Eu}^{2+}$ with a High Color Rendering Index for Solid State Lighting

Journal:	<i>Journal of Materials Chemistry C</i>
Manuscript ID	TC-ART-09-2020-004228.R2
Article Type:	Paper
Date Submitted by the Author:	19-Mar-2021
Complete List of Authors:	Takeda, Takashi; National Institute for Materials Science, Funahashi, Shiro; National Institute for Materials Science Xie, Rong-Jun; Xiamen University, College of Materials Hirosaki, Naoto; National Institute for Materials Science, Nano Ceramics Center

ARTICLE

Broadband White Luminescent Phosphor $\text{Ba}(\text{Si}_{7-x}\text{Al}_x)\text{Li}_y(\text{N}_{10-x+y}\text{O}_{x-y})\text{:Eu}^{2+}$ with a High Color Rendering Index for Solid State Lighting

Takashi Takeda,^{*a} Shiro Funahshi,^a Rong-Jun Xie^b and Naoto Hirosaki^a

Received 00th January 20xx,
Accepted 00th January 20xx

DOI: 10.1039/x0xx00000x

Analysis of a mixture product from Ba_3N_2 , Si_3N_4 , AlN , Li_3N , and EuN reveals a broadband white luminescent particle $\text{Ba}(\text{Si}_{7-x}\text{Al}_x)\text{Li}_y(\text{N}_{10-x+y}\text{O}_{x-y})\text{:Eu}^{2+}$. It shows a high color rendering index value of 90 despite being an Eu^{2+} only doped material. The emission spectrum at a low temperature of -190°C can be decomposed into three Gaussian profiles, indicating a crystal structure with three unique Eu coordination spheres. Single crystal XRD analysis shows that the single Ba site in $\text{Ba}(\text{Si}_{7-x}\text{Al}_x)(\text{N}_{10-x}\text{O}_x)$ splits into three Ba sites. From the chemical analysis and bond valance sum map of the Li ion, we estimate that Li intrudes into the $\text{Ba}(\text{Si}_{7-x}\text{Al}_x)(\text{N}_{10-x}\text{O}_x)$ lattice and shifts some Ba from its original position to two new Ba sites. This is a unique approach where a new phosphor is obtained by introducing a small cation into a known crystal structure.

Introduction

Phosphor converted white LEDs (pc-wLEDs) are entering into the lighting market due to their high efficiency, environmental friendliness, compactness, light weight, and long lifetime. Currently, $\text{Y}_3\text{Al}_5\text{O}_{12}\text{:Ce}^{3+}$ (YAG:Ce³⁺) and related garnet-type materials are the most prevalent LED phosphors.¹ However, pc-wLEDs using YAG:Ce emit bluish-white with a poor color rendering index. To compensate for the red components, nitride and oxynitride phosphors²⁻⁶ are mixed with YAG:Ce³⁺. Consequently, pc-wLEDs emitting warm white light with a high color rendering index are commercialized.

Recently Li-containing nitride and oxynitride phosphors have been reported to show an interesting luminescence property and crystal structure (i.e., a narrow-band emission such as $(\text{Sr,Ca})\text{LiAl}_3\text{N}_4\text{:Eu}^{2+}$,^{7,8} $\text{BaLi}_2\text{Al}_2\text{N}_2\text{N}_6\text{:Eu}^{2+}$,⁹ $\text{Ba}_2\text{LiAlSi}_7\text{N}_{12}\text{:Eu}^{2+}$,¹⁰ $\text{SrLi}_2\text{Al}_2\text{O}_2\text{N}_2\text{:Eu}^{2+}$,¹¹ $\text{Sr}_4\text{LiAl}_{11}\text{N}_{14}\text{:Eu}^{2+}$,¹² $\text{Li}_2\text{Ca}_2\text{Mg}_2\text{Si}_2\text{N}_6\text{:Eu}^{2+}$ ¹³ and a supertetrahedron consisting of 35 AlN_4 units such as $\text{Ca}_{18.74}\text{Li}_{10.5}\text{Al}_{39}\text{N}_{55}\text{:Eu}^{2+}$ ¹⁴). The ionic size of Li is between large constitution elements (i.e., Ba, Sr, Ca, La) and small constitution elements (Si, Al). Li can occupy independent crystallographic sites and contribute to a variety of crystal structures. Further discovery of interesting Li-containing phosphors are anticipated. To analyze the crystal structure and luminescence properties of new phosphors, a single phase (nearly single phase) powder is necessary. However, the Li component easily evaporates during synthesis, and the Li composition is difficult to control. Fabricating a single-phase powder of a new phosphor by adjusting the composition and synthetic conditions is a time-consuming and burdensome process. An effective alternative is to analyze one particle. We have developed an efficient method to find new phosphors from a mixture powder synthesized by a standard process.¹⁵ Our method is named the

“Single Particle Diagnosis Approach”. Even if the powder product is not a single phase, it can be treated as a single phase and a single crystal by considering each isolated particle. In our research, we select a single particle from the mixture product and analyze its crystal structure and the luminescence properties (emission and excitation spectra, temperature dependence, and quantum efficiency (QE), and decay).

In this paper, a broadband white luminescent phosphor particle $\text{Ba}(\text{Si}_{7-x}\text{Al}_x)\text{Li}_y(\text{N}_{10-x+y}\text{O}_{x-y})\text{:Eu}^{2+}$ is discovered in a mixture product from Ba_3N_2 , Si_3N_4 , AlN , Li_3N , and EuN . Crystal structure and chemical analyses indicate that the anomalous broadband emission is due to Li intrusion into the crystal lattice, which produces multiple Ba sites for Eu doping.

Experimental

Starting materials of Ba_3N_2 (Materiaon, 99.7%), EuN (Materiaon 99.9%), Si_3N_4 (Ube, E10), AlN (Tokuyama, E-grade), and Li_3N (Kojundo Chemical, 2N) were mixed in a cation molar ratio of $\text{Ba}:\text{Eu}:\text{Si}:\text{Al}:\text{Li} = 0.80:0.20:0.58:6.42:3.00$ in a glove box under a nitrogen atmosphere (M-Braun). The mixture was filled in a boron nitride crucible and fired in a nitrogen atmosphere of 0.92 MPa at 1900°C for 2 h (Fujidempa Kogyo, FVPHR-R-10, FRET-40). The product was irradiated by 370-nm UV LED light in air, and a white luminescent particle was selected under microscopic observation. The particle was mounted at the top of a glass capillary with glue. The single crystal XRD data of the single particle were collected using a diffractometer (Bruker-AXS, SMART APEX II Ultra) with $\text{Mo K}\alpha$ radiation ($\lambda = 0.71073 \text{ \AA}$) and multilayer focusing mirrors as a monochromator operating at 50 kV and 50 mA. The absorption corrections were applied using the multiscan procedure SADABS.¹⁶ The crystal structure was solved by direct methods implemented in SHELXL-97.¹⁷ The crystal structure was refined with anisotropic displacement parameters by the full-matrix least-squares calculation on F^2 in SHELXL-2013.¹⁷ Elemental analysis was conducted using a scanning electron microscope (Hitachi High-technology, SU1510) equipped with an energy dispersive spectroscopy instrument (Bruker AXS, XFlash SDD) operated at 15 kV. The Li/Si ratio was analyzed by laser ablation inductively

^a Sialon Group, National Institute for Materials Science, Tsukuba 305-0044, Japan

^b College of Materials, Xiamen University, Simingnan-Road 422, Xiamen 361005, China

Electronic Supplementary Information (ESI) available: [details of any supplementary information available should be included here]. See DOI: 10.1039/x0xx00000x

coupled plasma mass spectrometry (LA-ICP-MASS) with He as the carrier gas (Cyber Laser, IFRIT and ThermoFisher, ELEMENT XR) using LiSi_2N_3 (laboratory made), NIST1834, and BCR126A as standard materials. To determine the valence of Eu, microbeam X-ray absorption fine structure (XAFS) analysis was carried out at the BL14B2 beamline of the SPring-8 synchrotron radiation facility (Hyogo, Japan).

The luminescent properties of a single particle (emission and excitation spectra, temperature dependence, quantum efficiency, decay) were measured using microspectroscopic methods. The details are described in the previous paper.^{10,15}

Results and discussion

Characteristics of white luminescent particles

Various emission colors are observed under UV radiation (Figure 1(a)). In particular, several types of white luminescent particles (bluish-white, white, and yellowish-white) appear (Figure 1(b)–(d)). The yellowish-white particle is larger than the other particles, and it is formed as a parallelepiped shape with dimensions of $120 \mu\text{m} \times 50 \mu\text{m} \times 20 \mu\text{m}$. Figure 1(e) shows the PL spectra of white luminescent particles excited by 370-nm light. All particle samples show a broad emission spectrum (Figure 1(e)). The blueish-white luminescent particle has a peak around 490 nm and a shoulder around 570 nm. On the other hand, the white and yellowish-white luminescent particles display a peak around 570 nm and a shoulder around 470 nm. The spectra cover the whole visible range from 400 nm to 800 nm. The Commission International de l'Éclairage (CIE) chromaticity coordinates (x,y) and the correlated color temperature (CCT) based on the emission

spectrum are (0.2756, 0.3460) and 8367K for the bluish-white luminescent particle (Figure 1(f)). For the white and yellowish-white luminescent particles, they are (0.3212, 0.3878) and 5914K and (0.3603, 0.4222) and 4769K, respectively. The chromaticity coordinates are all near a Planckian locus. The color rendering index (Ra) of the bluish-white, white, and yellowish-white luminescent particles are 87.2, 88.5 and 82.7, respectively. It is surprising that one particle of the phosphor shows such a broadband white emission with a high Ra value. Typically phosphors with different emission spectra (i.e., blue, green, and red phosphors) are mixed to obtain a broadband luminescence spectrum such as those applied to the near UV-type white LEDs.¹⁸ Another way to generate broadband white emission with a high Ra value is to use several kinds of luminescent centers where each has its own luminescence property in the same host structure.^{19,20} Herein only Eu is used as a luminescent center. To determine the valence of the doped Eu, microbeam XAFS analysis of the Eu L_3 edge was carried out in the fluorescence mode for the yellowish-white luminescent particle. Figure 2 shows the X-ray absorption near edge structure (XANES) region. Although the S/N is low, a clear absorption corresponding to Eu^{2+} is observed at approximately 6972 eV.

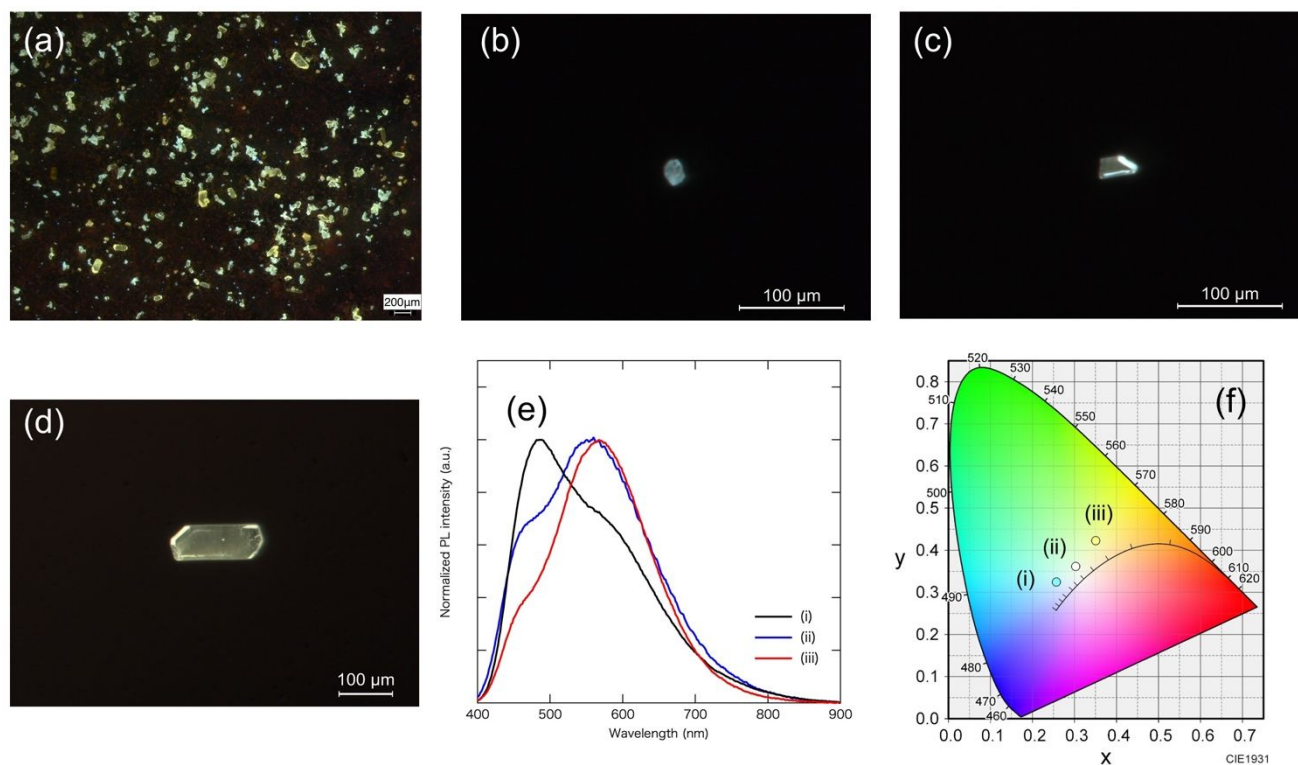


Figure 1 Photographs under UV light of (a) the product generated from a molar ratio of Ba:Eu:Si:Al:Li = 0.80:0.20:0.58:6.42:3.00, (b) a bluish-white luminescent particle, (c) a white luminescent particle, and (d) a yellowish-white luminescent particle. (e) Emission spectra of (i) the bluish-white luminescent particle, (ii) the white luminescent particle, and (iii) the yellowish-white luminescent particle excited by 370-nm light. The small oscillation of (ii) is due to light interference. (f) Chromaticity coordinates of (i) the bluish-white luminescent particle, (ii) the white luminescent particle, and (iii) the yellowish-white luminescent particle.

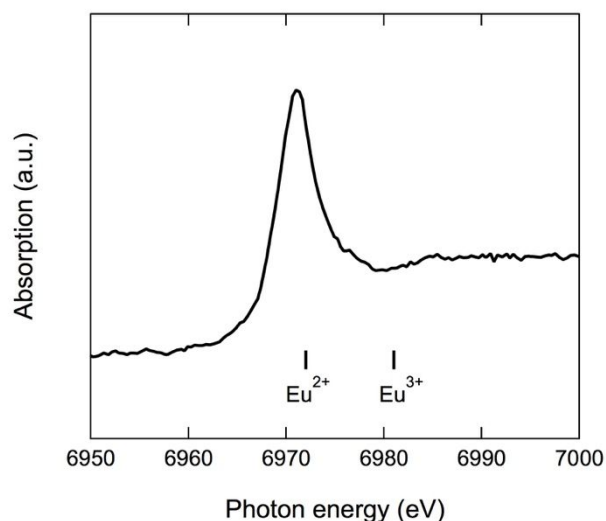


Figure 2 Eu L3 XANES spectrum of one yellow-white luminescent particle. Ticks denote the positions of Eu^{2+} and Eu^{3+} .

The particles seem to be a single crystal. However, there is a possibility of agglomeration of different luminescent particles. Single crystal XRD analysis was performed for the yellowish-white luminescent particle. It is a single crystal without contamination of other luminescent particles, and the crystal structure is the same type as $\text{BaSi}_7\text{N}_{10}$.²¹ (A monoclinic unit cell of $a = 6.8911(5)$ Å, $b = 6.7047(5)$ Å, $c = 9.6827(7)$ Å, and $\beta = 106.212(1)^\circ$ with the Pc space group (No. 7)). The crystal in Figure 1(d) reflects the monoclinic β angle. EDS analysis of the particle indicates the presence of Al and Eu (Si:Al = 6.66:0.34, Ba:Eu = 0.81:0.19), with a composition of $\text{Ba}_{0.81}\text{Eu}_{0.19}(\text{Si}_{6.66}\text{Al}_{0.34})(\text{N}_{9.66}\text{O}_{0.34})_{10}$ ($\text{Ba}(\text{Si}_{7-x}\text{Al}_x)(\text{N}_{10-x}\text{O}_x):\text{Eu}^{2+}$) with oxygen for charge compensation, similar to other nitridosilicates. Although the nominal composition of the starting materials lacks oxygen, a small amount of oxide impurities (~1 wt%) is inevitably included in the nitride starting materials (AlN , Si_3N_4). These oxide impurities can be included in the particle. Eu^{2+} doped $\text{BaSi}_7\text{N}_{10}$ powder shows a blue emission peak around 475 nm.²² The emission wavelength changes with the Eu concentration and Al/O substitution. The emission around 470 nm seems to correspond to the emission from $\text{Ba}(\text{Si}_{7-x}\text{Al}_x)(\text{N}_{10-x}\text{O}_x):\text{Eu}^{2+}$. To check the luminescence of $\text{Ba}(\text{Si}_{7-x}\text{Al}_x)(\text{N}_{10-x}\text{O}_x):\text{Eu}^{2+}$, $\text{Ba}_{0.81}\text{Eu}_{0.19}(\text{Si}_{6.66}\text{Al}_{0.34})(\text{N}_{9.66}\text{O}_{0.34})_{10}$ was prepared from Ba_3N_2 , EuN , Si_3N_4 , AlN and Al_2O_3 in the same firing condition. The $\text{Ba}_{0.81}\text{Eu}_{0.19}(\text{Si}_{6.66}\text{Al}_{0.34})(\text{N}_{9.66}\text{O}_{0.34})_{10}$ particle showed a blue emission peak around 470 nm and there was no shoulder at the longer wavelength side (Figure S1).

Origin of the broadband white luminescence

To investigate the origin of the broadband white luminescence, especially for the longer wavelength side, the emission spectrum for the yellowish-white luminescent particle was measured at low temperatures of -100 °C and -190 °C (Figure 3(a)). The shoulder around 460 nm is more distinct at -100 °C, and becomes an apparent peak at -190 °C. The main peak around 570 nm shifts to a longer wavelength. The spectrum at -190 °C can be fitted by a three-component Gaussian curve (peak positions: 2.09 eV, 2.46 eV, 2.71 eV) (Figure 3(b)), indicating that Eu has three different environments. However, the crystal structure of $\text{Ba}(\text{Si}_{7-x}\text{Al}_x)(\text{N}_{10-x}\text{O}_x)$

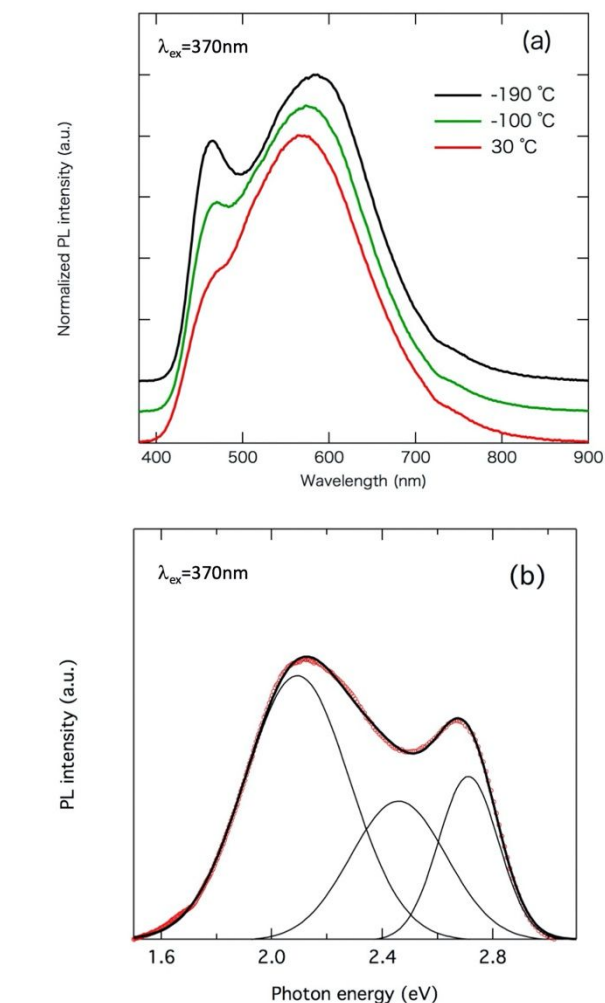


Figure 3 (a) Normalized emission spectra of one yellow-white luminescent particle at RT (red), -100 °C (green), and -190 °C (black). (b) Emission spectrum of one yellow-white luminescent particle at -190 °C is decomposed by three Gaussian components in an energy scale.

$\text{Ba}(\text{Si}_{7-x}\text{Al}_x)(\text{N}_{10-x}\text{O}_x)$ has one crystallographic Ba site for Eu doping, and there is no another large space for Eu in the crystal structure. A structural change to produce the three Ba sites is anticipated in $\text{Ba}(\text{Si}_{7-x}\text{Al}_x)(\text{N}_{10-x}\text{O}_x)$.

In $\text{Ba}(\text{Si}_{7-x}\text{Al}_x)(\text{N}_{10-x}\text{O}_x)$, corner- and edge-sharing SiN_4 tetrahedra form a three-dimensional network (Figure 4(a)). Ba occupies the site coordinated by twelve anions (Figure 4(b)). To obtain the information about the three Ba sites from diffraction analysis, the residual electron densities (Fo-Fc) were calculated. Residual electron densities are observed at the two positions near the Ba site (Figure 4(c)). The residual densities were analyzed using the split atom model depicted in Figure 4(d), where Ba1 (green ball) is the original site and Ba2 (red ball) / Ba3 (blue ball) are the new sites. The occupancies of the Ba1, Ba2, and Ba3 sites are 0.706(4), 0.154(4), and 0.140(4), respectively, and the occupancy of Ba2 is close to the Ba3 site. The $R[F_2 > 2\sigma(F_2)]$ and $wR(F_2)$ values decrease from 0.0293 and 0.0729 to 0.0173 and 0.0443, respectively. The supporting information shows the crystallographic data, atomic coordinates, isotropic displacement parameters, site occupancies, and anisotropic displacement parameters (Table S1-S3). The Ba:Eu, Si:Al, and N:O ratios in

each site are fixed to the ratios in the $\text{Ba}_{0.81}\text{Eu}_{0.19}(\text{Si}_{6.66}\text{Al}_{0.34})(\text{N}_{9.66}\text{O}_{0.34})_{10}$ composition. Because the Ba3 site is close to the Ba1 site (0.31 Å), refining the anisotropic displacement parameters of Ba3 site is difficult. On the other hand, the residual electron density near the Ba site was not observed in the blue luminescent $\text{Ba}_{0.81}\text{Eu}_{0.19}(\text{Si}_{6.66}\text{Al}_{0.34})(\text{N}_{9.66}\text{O}_{0.34})_{10}$ particle synthesized without Li_3N (Table S4-S6). Due to the small crystal size, it was difficult to refine the anisotropic displacement parameters in some anion sites.

luminescence spectra were measured. We used particles with similar luminescence spectra as shown in Figure 1(e)-iii. Figure 5 shows that the outward form of the fired particles does not change. On the other hand, the emission spectra obviously changes. In the particle fired at 1200 °C, the yellow-white luminescence turns into bluish-white luminescence. In the emission spectra normalized by the excitation intensity, the intensity around 570 nm largely decreases. The Li:Si ratio decreases from 0.013 before firing to 0.005 after firing. In the particle heated at 1500 °C, the emission

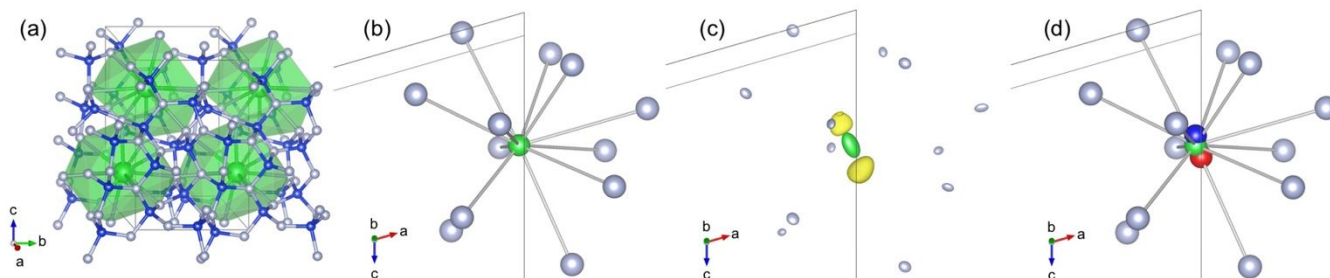


Figure 4 (a) Crystal structure of $\text{Ba}(\text{Si}_x\text{Al}_x)(\text{N}_{10-x}\text{O}_x)$. Green polyhedra are BaN_{12} . Green spheres are Ba, blue spheres are (Si, Al), and white spheres are (N, O). (b) Coordination sphere of the Ba site. (c) Residual electron densities around the Ba site. Isosurface level is $2.4 \text{ e}/\text{\AA}^3$. Atoms are drawn as displacement ellipsoids (50% probability level). (d) Coordination sphere of the Ba sites in the split atom model. Green, red, and blue spheres indicate Ba1, Ba2, and Ba3, respectively. Crystal structure images are drawn with the program VESTA.²³

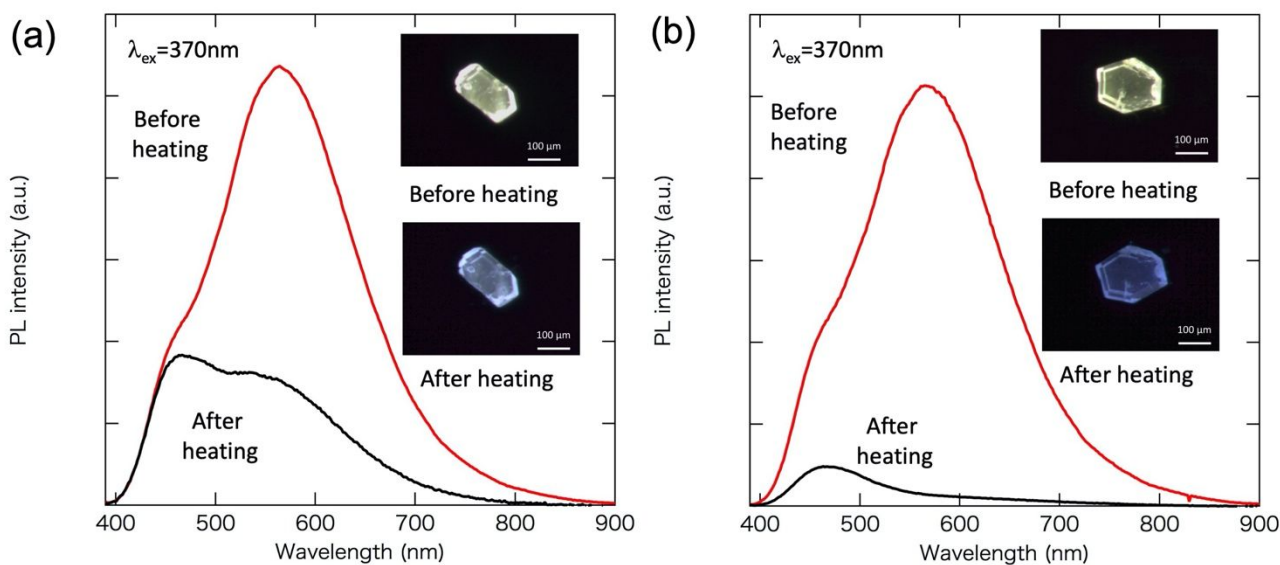


Figure 5 Difference in the emission spectra and the appearance of one yellow-white luminescent particle by firing at (a) 1200 °C and (b) 1500 °C.

The three Ba sites correspond to an emission spectrum composed of three Gaussian components. However, the reason that the two new Ba sites form is unclear. In the synthesis of the white luminescent particles, Li_3N is included in the starting materials. It is possible that the Li taken into the crystal lattice splits the Ba site. LA-ICP-MASS was used to detect and analyze the amount of Li in the yellowish-white luminescent particle. The particle contains Li at a Li:Si ratio of 0.0109. Hence, the particle composition is $\text{Ba}_{0.81}\text{Eu}_{0.19}\text{Li}_{0.11}\text{Si}_{6.66}\text{Al}_{0.34}\text{O}_{0.23}\text{N}_{9.77}$ ($\text{Ba}(\text{Si}_{7-x}\text{Al}_x)\text{Li}_y(\text{N}_{10-x+y}\text{O}_{x-y})\text{:Eu}^{2+}$). To verify that the incorporated Li affects the luminescence property, the yellow-white luminescent particles were re-fired at 1200 °C and 1500 °C in a nitrogen atmosphere of 0.92 MPa for 2 h. Then the Li content and

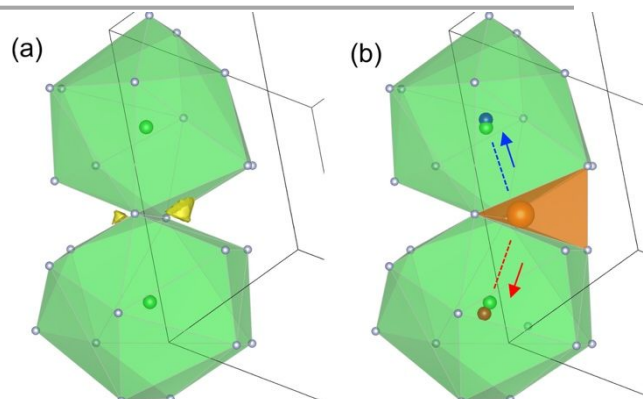


Figure 6 (a) BVS map of $\text{BaSi}_7\text{N}_{10}$ for a Li ion with an isosurface level of ± 0.2 valence units. BaN_{12} polyhedron are shown. (b) Estimated Ba movement by positioning Li (orange ball) at the candidate position. Green, red, and blue balls denote Ba1, Ba2, and Ba3 sites, respectively.

around 570 nm nearly disappears and a low-intensity emission at 460 nm appears. The Li:Si ratio decreases from 0.013 before firing to 0.0 after firing. To check how the crystal structure changed by refiring, the crystal structure of the refired particle at 1500 °C was analyzed. The split of Ba site disappeared and it was analyzed by the single Ba site model (Table S7-S9). These results suggest that the incorporated Li is related to the emission around 570 nm. Hence, the different emission spectra shown in Figure 1(e) are attributed to the Li content in the particles.

BaLi₂Al₂Si₂N₆:Eu²⁺, 3.62 Å in Ba₂LiAlSi₇N₁₂:Eu²⁺). If Li occupies the position, the two near Ba will move away from the Li site, as shown by the arrows. The red and blue balls are the two new Ba sites obtained in the XRD analysis. These new Ba sites are situated at the extension of the dotted lines. Indeed, structural relaxation of other atoms, including the Li tetrahedra, should occur. Because Ba is pushed away, the sizes of the coordination spheres of the new Ba sites should be smaller than that of the original Ba site. This causes the large crystal field splitting of Eu²⁺ 5d levels and shifts

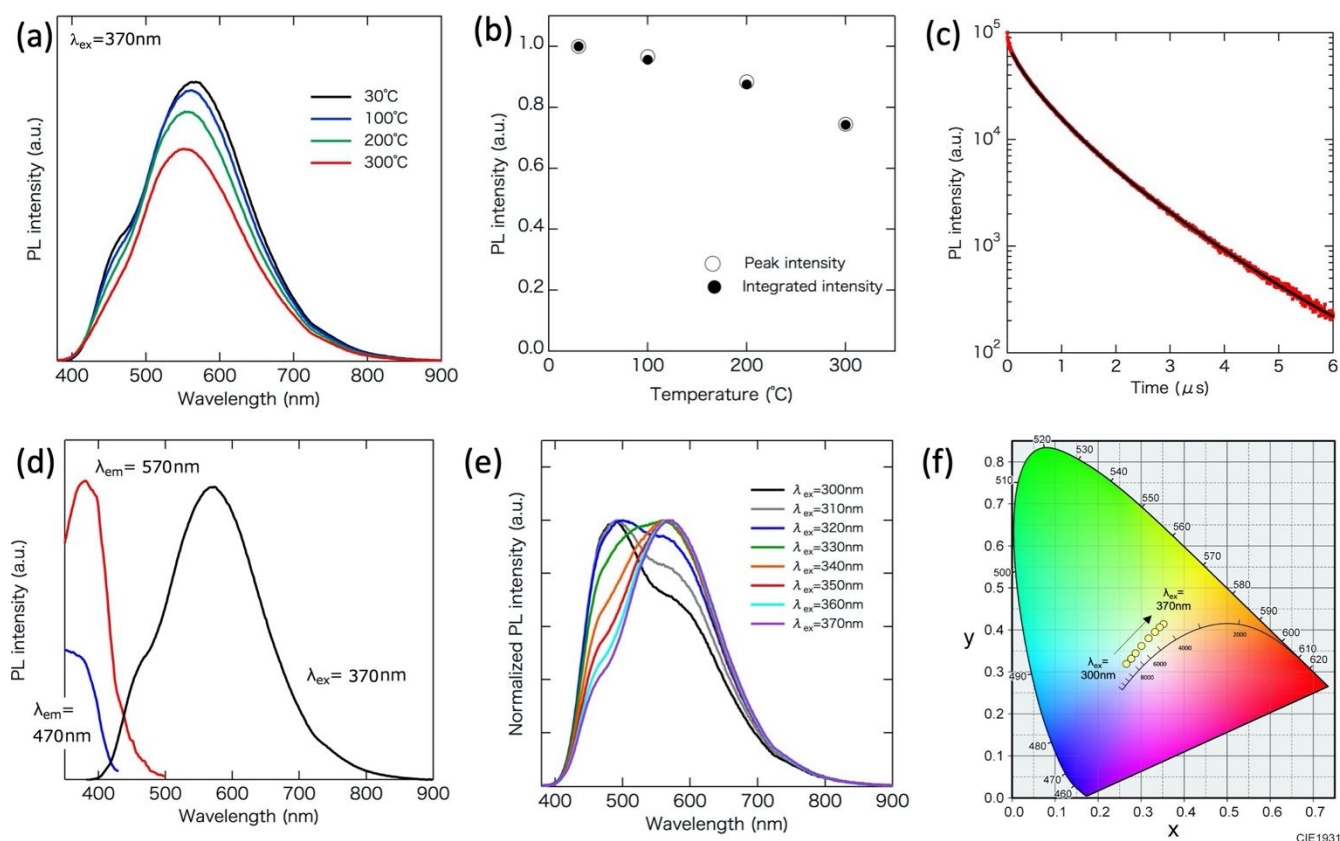


Figure 7 Luminescence properties of one yellowish-white luminescent particle. (a) Temperature dependence of the emission spectra in the temperature range from 30 °C to 300 °C. (b) Temperature dependence of the peak intensity (open circle) and integrated intensity (filled circle). (c) Observed (red dots) and fitted (black line) emission decay curves for the excitation of 376-nm pulsed light. (d) Excitation (monitored at 470 nm and 570 nm) and emission (excited by 370 nm) spectra. (e) Emission spectra excited by different wavelengths from 300 nm to 370 nm. (f) CIE color coordinates excited by different wavelengths from 300 nm to 370 nm.

The Li ion is small and monovalent. If the crystal structure has enough space, the Li ion can occupy the position. Because the amount of Li in the particle is small, it is very difficult to obtain the Li position from the single crystal XRD analysis. The bond valence sum (BVS) map is commonly employed to estimate the possible Li diffusion path in a crystal structure of a Li ion conductive material.^{24,25} Here, we used this method to estimate the Li occupiable position in the crystal structure. The calculation was carried out at a 0.1 Å resolution by the program BondStr in the FullProf suite. For simplicity, non-substituted BaSi₇N₁₀ was used. Two spatial regions near BaN₁₂ polyhedron are obtained as Li occupiable positions (Figure 6(a)). We selected the wider region as the candidate position. When Li is placed at the center of the candidate position, it is coordinated by four nitrogen atoms, as shown as orange tetrahedra in Figure 6(b). The distances from the Li to the nearest Ba (green balls) are 2.60 Å (red dotted line) and 2.82 Å (blue dotted line). These are apparently shorter than those of the other Ba containing nitridolithoaluminosilicates (3.26 Å in

the emission wavelength to the longer wavelength side. The occupancies of the Ba2 and Ba3 sites obtained by XRD analysis are similar (0.154(4), 0.140(4)), supporting the estimation. The XRD analysis by positioning Li to the estimated site does not improve the R value, which is probably due to the small amount of Li. Hence, it is necessary to experimentally elucidate the Li position by a neutron diffraction technique that includes another spatial region obtained in the BVS map. Because Li intrusion into the crystal lattice makes the local structure electropositive, the local structure should have an Al or O rich composition to maintain charge neutrality. Such local disorder may have some effect on the broadening of the emission spectra. The PL intensity decrease by refiring will be due to the formation of defect by Li desorption.

Luminescence properties

Luminescence properties of the yellowish-white luminescent particle were measured in detail using a microspectroscopic

method. Figure 7(a,b) show the temperature dependence of the emission spectra, peak intensity, and integrated intensity. As the temperature increases, the shoulder around 460 nm becomes weaker and almost disappears at 300 °C. One possible reason is an energy transfer from the high energy Eu site (Eu1) to the low energy Eu sites (Eu2 and Eu3). The peak intensity gradually decreases with temperature, and the peak intensities at 200 °C and 300 °C are 88% and 75% of the intensity observed at room temperature, respectively. At 200 °C and 300 °C, the integrated intensities are 88% and 74% of that at room temperature, respectively.

The internal quantum efficiency of the yellowish-white luminescent particle by 405-nm excitation is 30%. Eu²⁺-doped

Table 1 CIE chromaticity coordinates (x,y), correlated color temperature (CCT), and color rendering index (Ra) excited by 300–370 nm.

$\lambda_{\text{ex}} / \text{nm}$	300	310	320	330	340	350	360	370
x	0.2654	0.2765	0.2868	0.3004	0.3171	0.3320	0.3430	0.3517
y	0.3193	0.3316	0.3445	0.3619	0.3803	0.3952	0.4063	0.4141
CCT / K	9939	8662	7749	6851	6063	5529	5201	4973
Ra	89.5	90.4	90.0	88.7	85.8	85.8	84.5	83.8

excitation wavelength can control the emission spectrum. Figure 7 (e,f) show the emission spectra and CIE chromaticity coordinates as functions of the excitation wavelength. The intensity ratio of the 570-nm and 470-nm peaks changes with the excitation wavelength. The spectrum excited by 300 nm resembles the bluish-white luminescent particle in Figure 1(e). The spectrum excited by 350 nm resembles the white luminescent particle in Figure 1(e). Hence, both the excitation wavelength and Li content can control the intensity ratio of the 570-nm and 470-nm peaks. The CIE chromaticity coordinates continuously change near black body radiation. Table 1 lists the CIE chromaticity coordinates, correlated color temperature, and color rendering index (Ra). The Ra values reach 90 for the 310-nm and 320-nm excitations. For the 330-nm excitation, the CCT is close to daylight (6500K) with Ra = 88.7. In the 370-nm excitation, it is close to neutral white (5000K) with Ra = 83.8. Consequently, a high color rendering is attained from an Eu²⁺ only doped phosphor. Recently, Eu²⁺ only doped Sr₂AlSi₂O₆N has been reported to show a broadband emission.²⁹ In this case, the broadband emission is ascribed to the multiple local environments induced by the disordering in the crystal structure. Utilization of multiple sites is important to obtain a broadband emission from Eu²⁺ only doped material.

Conclusions

A broadband white luminescent particle Ba(Si_{7-x}Al_x)Li_y(N_{10-x+y}O_{x-y}):Eu²⁺ is discovered by analyzing the product from Ba₃N₂, Si₃N₄, AlN, Li₃N, and EuN. The luminescence spectrum of the particle at low temperature can be decomposed by three Gaussian profiles, indicating three different Eu coordination spheres in the structure. Single crystal XRD analysis shows the residual electron densities around the Ba site, which are well analyzed by the position of the three Ba sites (splitting atom model). From elemental analysis and the BVS map, it is estimated that Li intrusion into the Ba(Si_{7-x}Al_x)(N_{10-x}O_x):Eu²⁺ lattice shifts some Ba from its original position to two new Ba sites. The Li position could not be determined experimentally. Further studies are necessary to elucidate the Li position. The emission spectra cover the whole visible range and

BaSi₇N₁₀ shows a maximum emission intensity at Eu 8% and concentration quenching at a higher Eu doping amount.²⁶ Hence, altering the Eu concentration should improve the quantum efficiency. Figure 7(c) shows the emission decay of a yellowish-white luminescent particle excited by 376 nm. It is not a single exponential curve but is well fitted by the three exponentials (0.15 μ s (5%), 0.57 μ s (47%), and 1.31 μ s (48%)) coinciding with three Eu sites. The short decay time is due to the energy transfer from the high energy Eu site to the low energy Eu sites.^{27,28} Figure 7(d) shows the excitation spectra of the yellowish-white luminescent particle monitored at 570 nm and 470 nm. The spectral shape depends on the monitoring wavelength, which suggests that the

show a high color rendering index of 80 ~ 90. This is a unique approach where a new phosphor is obtained by introducing a small cation into a known structure. Hence, future studies employing this approach should discover new phosphors.

Conflicts of interest

There are no conflicts to declare.

Acknowledgements

The synchrotron radiation experiments were performed at BL14B2 of SPring-8 with the approval of the Japan Synchrotron Radiation Research Institute (JASRI) (Proposal No. 2015B1615). This work was partly supported by JST CREST Gant Number JPMJCR19J2, Japan.

Notes and references

- 1 S. Nakamura and G. Fasol, *The Blue Laser Diode: GaN Based Light Emitters and Lasers*, Springer, Berlin, 1997.
- 2 K. Uheda, N. Hirosaki, Y. Yamamoto, A. Naoto, T. Nakajima and H. Yamamoto, *Electrochem. Solid State Lett.*, 2006, **9**, H22-H25.
- 3 Y.Q. Li, J.E.J. van Steen, J.W.H. van Kreveld, G. Botty, A.C.A. Delsing, F.J. Disalvo, G. de With and H.T. Hintzen, *J. Alloys Compd.*, 2006, **417**, 273-279.
- 4 H.A. Hoppe, H. Lutz, P. Morys, W. Schnick and A.J. Seilmeier, *Phys. Chem. Solids*, 2000, **61**, 2001-2006.
- 5 R.J. Xie, N. Hirosaki, K. Sakuma, Y. Yamamoto and M. Mitomo, *Appl. Phys. Lett.*, 2004, **84**, 5404-5406.
- 6 Seto, T.; Kijima, N.; a, Hirosaki, N. A New Yellow Phosphor La₃Si₆N₁₁:Ce³⁺ for White LEDs. *ECS Transactions* 2009, **25**, 247-252.
- 7 Pust, P.; Weiler, V.; Hecht, C.; Tucks, A.;; Wochnik, A. S.; Henß, A. K.; Wiechert, D.; Scheu, C.; Schmidt, P. J.; Schnick, W. Narrow-band red-emitting Sr[LiAl₃N₄]:Eu²⁺ as a next-

- generation LED-phosphor material. *Nature Mat.* 2014, 13, 891-896.
- 8 Pust, P.; Wochnik, A. S.; Baumann, E.; Schmidt, P. J.; Wiecher, D.; Scheu, C.; Schnick, W. Ca[LiAl₃N₄]:Eu²⁺-A Narrow-Band Red-Emitting Nitridolithoaluminate. *Chem. Mater.* 2014, 24, 3544-3548.
- 9 Strobel, P.; Schmiechen, S.; Siegert, M.; Tücks, A.; Schmidt, P. J.; Schnick, W. Narrow-Band Green Emitting Nitridolithoalumosilicate Ba[Li₂(Al₂Si₂)N₆]:Eu²⁺ with Framework Topology whj for LED/LCD- Backlighting Applications. *Chem. Mater.* 2015, 27, 6109-6115.
- 10 Takeda, T.; Hirosaki, N.; Funahashi, S.; Xie, R. -J. Narrow-Band Green-Emitting Phosphor Ba₂LiSi₇AlN₁₂:Eu²⁺ with High Thermal Stability Discovered by a Single Particle Diagnosis Approach. *Chem. Mater.* 2015, 27, 5892-5898
- 11 Hoerder, G. J.; Seibald, M.; Baumann, D.; Schröder, T.; Peschke, S.; Schmid, P. C.; Tyborski, T.; Pust, P.; Stoll, I.; Bergler, M.; Patzig, C.; Reißaus, S.; Krause, M.; Berthold, L.; Höche, T.; Johrendt, D.; Huppertz, H. Sr[Li₂Al₂O₂N₂]:Eu²⁺-A high performance red phosphor to brighten the future. *Nat. Commun.* 2019, 10, 1824.
- 12 Wilhelm, D.; Baumann, D.; Seibald, M.; Wurst, K.; Heymann, G.; Huppertz, H. Narrow-Band Red Emission in the Nitridolithoaluminate Sr₄[LiAl₁₁N₁₄]:Eu²⁺. *Chem. Mater.* 2017, 29, 1204-1209.
- 13 Strobel, P., Weiler, V., Hecht, C., Schmidt, P. J. & Schnick, W. Luminescence of the narrow-band red emitting nitridomagnesosilicate Li₂(Ca_{1-x}Sr_x)₂[Mg₂Si₂N₆]: Eu²⁺ (x=0-0.06). *Chem. Mater.* 2017, 29, 1377-1383.
- 14 Wagatha, P.; Pust, P.; Weiler, V.; Wochnik, A. S.; Schmidt, P. J.; Scheu, C.; Schnick, W. Ca_{18.75}Li_{10.5}[Al₃₉N₅₅]:Eu²⁺ Supertetrahedron Phosphor for Solid- State Lighting. *Chem. Mater.* 2016, 28, 1220-1226.
- 15 Hirosaki, N.; Takeda, T.; Funahashi, A.; Xie, R. -J. Discovery of New Nitridosilicate Phosphors for Solid State Lighting by the Single-Particle-Diagnosis Approach. *Chem. Mat.* 2014, 26, 4280.
- 16 Sheldrick, G. M. SADABS, v. 2: Multi-Scan Absorption Correction; Bruker-AXS: WA, 2012.
- 17 Sheldrick, G. M. A short history of SHELX. *Acta Cryst.* 2008, A64, 112-122.
- 18 Sheu, J. K.; Chang, S. J.; Kuo, C. H.; Su, Y. K.; Wu, L. W.; Lin, Y. C.; Lai, W. C.; Tsai, J. M.; Chi, G. C.; Wu R. K. White-Light Emission From Near UV InGaN-GaN LED Chip Precoated With Blue/Green/Red Phosphors. *IEEE Photonics Technol. Lett.* 2013, 15, 18-20.
- 19 McKittrick, J.; Hannah, M. E.; Piquette, A.; Han, J. K.; Choi, J. I.; Anc, M.; Galvez, M.; Lugauer, H.; Talbot, J. B.; a, Mishra, K. C. Phosphor Selection Considerations for Near-UV LED Solid State Lighting. *ECS J. Solid State Sci. Technol.* 2013, 2, R3119-R3131.
- 20 Guo, N.;Zheng, Y.; Jia, Y.; Qiao, H.; †, You, H. Warm-White-Emitting from Eu²⁺/Mn²⁺-Codoped Sr₃Lu(PO₄)₃ Phosphor with Tunable Color Tone and Correlated Color Temperature. *J. Phys. Chem. C* 2012, 116, 1329-1334.
- 21 Huppertz, H.; Schnick, W. Edge-sharing SiN₄ Tetrahedra in the Highly Condensed Nitridosilicate BaSi₇N₁₀. *Chem. Eur. J.* 1997, 3, 249-252.
- 22 Li, Y. Q.; Delsing, A. C. A.; Metslaar, R.; de With G.; Hintzen, H. T. Photoluminescence properties of rare-earth activated BaSi₇N₁₀. *J. Alloys Compd.* 2009, 487, 28-33.
- 23 Momma, K.; Izumi, F. VESTA 3 for three-dimensional visualization of crystal, volumetric and morphology data. *J. Appl. Crystallogr.* 2011, 44, 1272-1276.
- 24 Adams, S.; Rao, R. P. High power lithium ion battery materials by computational design. *Phys. Status Solidi A.* 2011, 208, 1746-1753.
- 25 Xiao, R.; Li, H.; Chen , L. High-throughput design and optimization of fast lithium ion conductors by the combination of bond-valence method and density functional theory. *Sci. Rep.* 2015, 5, 14227.
- 26 Anoop, G.; Lee, D. W.; Suh, D. W.; Wu, S. L.; a Kang Min Ok, K. M.; Yoo, J. S. Solid-state synthesis, structure, second-harmonic generation, and luminescent properties of noncentrosymmetric BaSi₇N₁₀:Eu²⁺ phosphors. *J. Mater. Chem. C*, 2013, 1, 4705-4712.
- 27 Lee, S.; Sohn, K. S. Effect of inhomogeneous broadening on time-resolved photoluminescence in CaAlSiN₃:Eu²⁺. *Opt. Lett.*, 2010, 35, 1004-1006.
- 28 Wang, C. Y.; Takeda, T.; Kate, O. M.; Xie, R. J.; Takahashi K.; Hirosaki, N. Synthesis and photoluminescence properties of a phase pure green-emitting Eu doped JEM sialon (LaSi_{6-z}Al_{1+z}N_{10-z}O_z, z~1) phosphor with a large red-shift of emission and unusual thermal quenching behavior. *J. Mater. Chem. C*, 2016, 4, 10358-10366.
- 29 Li, S.; Xia, Y.; Amachraa, M.; Hung, N. T.; Wang, Z.; Ong, S. P.; Xie, R. J. Data-Driven Discovery of Full-Visible-Spectrum Phosphor. *Chem. Mater.* 2019, 31, 6286-6294.